Colloids and Surfaces A 537 (2018) 383–389

Contents lists available at ScienceDirect

Colloids and Surfaces A

journal homepage: www.elsevier.com/locate/colsurfa

Research Paper

Adsorption Behavior of Au(III) Complex Ion on Nickel Carbonate and Nickel Hydroxide

Hiroaki Ando[a], Daisuke Kawamoto[a,b,*], Hironori Ohashi[c], Tetsuo Honma[d], Tamao Ishida[e], Yoshihiro Okaue[a], Makoto Tokunaga[a], Takushi Yokoyama[a,*]

[a] Department of Chemistry, Faculty of Science, Graduate School of Kyushu University, 744 Motooka, Nishi-ku, Fukuoka 819-0395, Japan
[b] Department of Chemical and Biological Sciences, Faculty of Science, Japan Women's University, 2-8-1 Mejirodai, Bunkyo-ku, Tokyo 112-8681, Japan
[c] Faculty of Symbiotic Systems Science, Fukushima University, 1 Kanayagawa, Fukushima 960-1296, Japan
[d] Japan Synchrotron Radiation Research Institute (JASRI)/SPring-8, 1-1-1 Kouto, Sayo-gun, Hyogo 679-5198, Japan
[e] Research Center for Gold Chemistry, School of Urban Environmental Sciences, Tokyo Metropolitan University, 1-1 Minami-osawa, Hachioji, Tokyo 192-0397, Japan

GRAPHICAL ABSTRACT

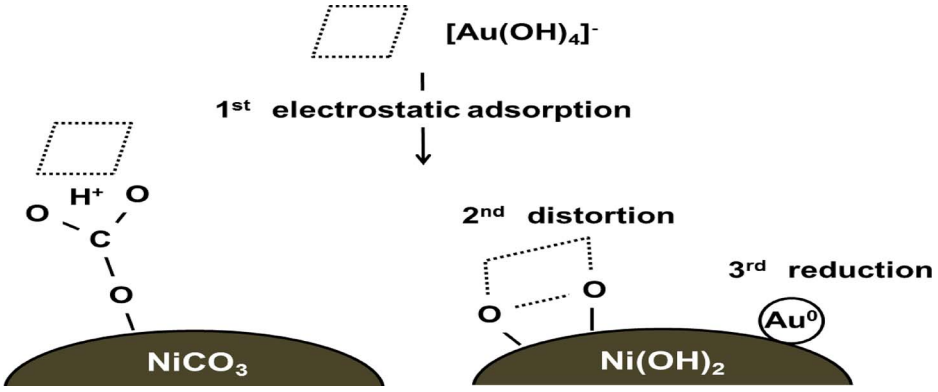

ARTICLE INFO

Keywords:
Adsorption behavior
$[Au(OH)_4]^-$
$NiCO_3$
$Ni(OH)_2$
Gold supported catalyst
XA spectroscopy

ABSTRACT

When preparing gold(Au) supported on NiO catalysts by the coprecipitation method, the chemical state of the coprecipitated Au differed when Na_2CO_3 and NaOH were used as the coprecipitating reagents. In this preparation using Na_2CO_3 and NaOH solutions, precursor of support metal was largely $NiCO_3$ and $Ni(OH)_2$, respectively. Therefore, the different chemical states of Au may be controlled by the interaction between the $[Au(OH)_4]^-$ and precursor of support metal. The aim of this study is to elucidate why the chemical state of Au differs when using $NiCO_3$ and $Ni(OH)_2$.

Adsorption experiments of $[Au(OH)_4]^-$ onto $NiCO_3$ or $Ni(OH)_2$ were performed. The Au concentration in the filtrate was determined by atomic absorption spectrometry (AAS). The chemical state of the adsorbed Au was examined by X-ray absorption(XA) spectroscopy.

The adsorption experiments suggested that the change in surface charge on $NiCO_3$ and $Ni(OH)_2$ electrostatically controls the adsorption of $[Au(OH)_4]^-$. The XA analysis indicated that the chemical state of $[Au(OH)_4]^-$ adsorbed on $NiCO_3$ is maintained because of electrostatic interactions, while some of the $[Au(OH)_4]^-$

* Corresponding authors. Current address: 2-8-1 Mejirodai, Bunkyo-ku, Tokyo 112-8681, Japan.
E-mail addresses: kawamotod@fc.jwu.ac.jp (D. Kawamoto), yokoyamatakushi@chem.kyushu-univ.jp (T. Yokoyama).

http://dx.doi.org/10.1016/j.colsurfa.2017.10.028
Received 14 July 2017; Received in revised form 10 October 2017; Accepted 13 October 2017
Available online 14 October 2017
0927-7757/

adsorbed on $Ni(OH)_2$ may be reduced to Au(0) due to specific adsorption-accompanying distortion of the square planar structure of the adsorbed $[Au(OH)_4]^-$.

1. Introduction

Since Haruta et al. [1] prepared gold(Au) nanoparticle supported catalysts that usefully oxidize CO to CO_2 at low temperatures, these catalysts have been vigorously investigated. When preparing these catalysts, a mixed solution of $HAuCl_4$ and a metal nitrate (Fe, Co, Ni) is rapidly introduced into a basic solution, such as Na_2CO_3 or NaOH, and stirred to form the coprecipitate (precursor). To prepare the catalyst, the precursor is heated at an optimum temperature (300–500 °C) to reduce the coprecipitated $Au(OH)_3$ to Au(0) in addition to converting the metal hydroxide or metal carbonate to metal oxide. This method is called the "coprecipitation method". Because of its simplicity and convenience, the coprecipitation method is commonly used.

There are many studies about the characterization and catalytic activity of Au nanoparticles supported catalysts, but only a few reports have been published on their precursors. Although some basic solutions have been used as coprecipitating reagents in the coprecipitation method [2–5], no paper has been published on the effect of the coprecipitating reagent on the chemical properties of the precursor. We previously reported that when a Au nanoparticle supported catalyst was prepared by the coprecipitation method, the chemical state of the coprecipitated Au differed when using Na_2CO_3 and NaOH solutions as the coprecipitating reagents [6]. When using Na_2CO_3 and NaOH solutions, the support compounds were largely $NiCO_3$ and $Ni(OH)_2$, respectively. The results indicated that the different chemical states of Au may be controlled by the interaction between the Au(III) complex ions and each support compound. To elucidate why the chemical state of Au is different when $NiCO_3$ or $Ni(OH)_2$ are the support compounds, we investigated in further detail the adsorption behavior of Au(III) complex ions on $NiCO_3$ and $Ni(OH)_2$. Because of their importance in a variety of fields, many investigations have been conducted into the adsorption behavior of Au(III) complex ions on metal hydroxides and oxides [7–10]. However, no report has been published about the adsorption behavior of Au(III) complex ions on metal carbonates. This paper compares the adsorption behavior on $NiCO_3$ and $Ni(OH)_2$. As a Au/NiO catalyst has been practically used for the oxidation of CO and alcohols, nickel ion was selected as the metal ion in this study. It should be emphasized that different Au chemical states and different support compounds for the precursor may affect the Au particle size on the catalyst that controls the catalytic activity.

2. Experimental

2.1. Chemicals and sample solutions

All reagents used in this study were of analytical grade. All sample solutions were prepared with deionized-distilled water. Tetrachloroaurate-tetra-hydrate ($HAuCl_4{\cdot}4H_2O$) as an initial Au source was purchased from Tanaka Kikinzoku Kogyo K. K. Potassium tetrachloroaurate-n-hydrate ($K[AuCl_4]{\cdot}nH_2O$) for use as a Au(III) standard with an Au-Cl bond for X-ray absorption(XA) spectroscopy was purchased from Wako Pure Chemical Industries, Ltd. Gold(III) hydroxide ($Au(OH)_3$) as a Au(III) standard with an Au-O bond was prepared according to the literature [11,12]. $NiCO_3$ as an adsorbent was purchased from Wako Pure Chemical Industries, Ltd. $Ni(OH)_2$ as an adsorbent was prepared stoichiometrically by mixing a $Ni(NO_3)_2$ solution (1000 cm^3, [Ni] = 54 mmol dm^{-3}) and a NaOH solution (100 cm^3, 2.0 mol dm^{-3}) (Ni: OH = 1: 2). The precipitate was centrifuged, and the separated precipitate was suspended in water. The suspension was stirred for 12 h to remove $NaNO_3$. The precipitate was centrifuged again to separate it, and the precipitate was dried in a desiccator to obtain pure $Ni(OH)_2$. Crystalline $Ni(OH)_2$ as a standard was also purchased from Wako Pure Chemical Industries, Ltd. to compare with the synthesized $Ni(OH)_2$.

2.2. Adsorption experiment

$HAuCl_4$ solution (10, 20 and 50 ppm as Au, 500 cm^3) with 0.01 mol dm^{-3} of $NaNO_3$ was adjusted to the desired pH with NaOH solution and/or HNO_3 and stirred magnetically for 1 h to reach an equilibrium with respect to the formation of $[AuCl_n(OH)_{4-n}]^-$ (substitution of Cl^- with OH^- in the $[AuCl_4]^-$ complex ion). $NiCO_3$ or $Ni(OH)_2$ powder (500 mg) was added into the solution, and the suspension was stirred. During the adsorption experiment, the pH was monitored as it shifted to acid side. At appropriate intervals, an aliquot of the suspension was taken out and filtered with a 0.45 μm membrane filter. After filtration of the suspension, the pH was readjusted to the desired level. The Au concentration of the filtrate was determined by atomic absorption spectrometry (AA-6300, Shimadzu). The relative error of the Au determination by AAS was within 4.14%. After 24 h, the remaining suspension was filtered with a 0.45 μm membrane filter. The $NiCO_3$ or $Ni(OH)_2$ adsorbing Au (solid sample) on the filter was freeze-dried.

2.3. X-ray diffraction (XRD) measurements

XRD patterns of $NiCO_3$, synthesized $Ni(OH)_2$ and crystalline $Ni(OH)_2$ were measured using an Ultima IV, Rigaku at a scanning rate of 2° min^{-1} and a sampling angle interval of 0.02° in the 2θ range 10–65° with Cu Kα radiation (λ = 0.151478 nm). The operating voltage and current were 40 kV and 30 mA. Crystalline phases were identified by matching the diffraction patterns to ICDD powder diffraction files.

2.4. Measurement of zeta potential

$NiCO_3$ or $Ni(OH)_2$ were suspended in water, and the pH was adjusted to the desired level in the range from 7 to 11. The suspension was allowed to stand until large particles sank to the bottom of the vessel. The supernatant was used to measure the zeta potential of the $NiCO_3$ or $Ni(OH)_2$ particles. The measurement was conducted using a Zetasizer Nano ZSP ZEN5600, Malvern.

2.5. Measurement of XA spectra

The Au L_3-edge XA spectra for Au adsorbed on $NiCO_3$ or $Ni(OH)_2$ were measured at BL14B2 of SPring-8 (Hyogo, Japan) using a Si(311) double crystal monochromator with a Rh coated mirror. The X-ray absorption fine structure (XAFS) data for the standard materials ($KAuCl_4{\cdot}\ nH_2O$, $Au(OH)_3$ and Au foil) were collected under ambient conditions in the transmission mode and the transmitted X-ray was detected by an ion chamber. The standard materials were diluted with boron nitride (BN), and the diluted standard materials were made into pellets and placed in a polyethylene bag. The XAFS data for the solid samples were collected under ambient conditions in the fluorescence mode and the fluorescent X-ray was detected by the 19-element Ge-SSD. The spectral analysis was performed using the Athena software [13]. The extraction of the extended X-ray absorption fine structure (EXAFS) oscillation from the spectra, normalization by edge-jump and Fourier transformation were performed using the Athena software.

2.6. Transmission electron microscopy (TEM) observation

The catalytic activity of supported Au depends on the size distribution of Au on the metal oxide. Because the precursor is heated at an optimum temperature to synthesize the catalyst, the chemical state of Au in the precursor is a key to synthesize the catalyst. To examine the relationship between the support compound of precursor ($NiCO_3$ or $Ni(OH)_2$) and the particle size of Au in the Au/NiO catalyst, the TEM observation was performed for two samples. One is the sample prepared by adsorbing $[Au(OH)_4]^-$ (initial Au concentration: 20 ppm) on $NiCO_3$ for 24 h and by heating at 300 °C and another is the sample prepared by adsorbing $[Au(OH)_4]^-$ (initial concentration: 10 ppm) on $Ni(OH)_2$ for 24 h and by heating at 300 °C. To analysis the size of that, TEM observation was carried out using HR TEM operated at an accelerating voltage of 200 kV. The TEM specimens were prepared by dispersing the sample into water. The suspended solution was put on a holey carbon mesh supported by a Cu grid and air-dried.

3. Results and discussion

3.1. Chemical formulae of Au(III) complex ions in aqueous solution

The $[AuCl_4]^-$ complex ion can be present stably under strongly acidic conditions. Under weakly acidic to basic conditions, the Cl^- in the $[AuCl_4]^-$ complex ion is substituted with OH^- to form the $[AuCl_{4-n}(OH)_n]^-$ complex ions ($0 \le n \le 4$). The substitution reaction proceeds with increasing pH [14–16]. For the adsorption experiment with Au(III) complex ion, it is important to specify the chemical species present under the experimental conditions. Fig. 1 shows the distribution curve for each Au(III) complex ion in the pH range from 0 to 8 in a 0.01 mol dm^{-3} $NaNO_3$ solution at 25 °C. This curves were calculated according to the literature [14,17]. The solid line and dotted line indicate the distributions at total Au concentrations of 20 ppm and 50 ppm, respectively. Above pH 7, most of the Au(III) complex ions are present as $[Au(OH)_4]^-$. This is the species considered to be adsorbed on $NiCO_3$ or $Ni(OH)_2$ under the experimental conditions of this study.

3.2. $NiCO_3$ and $Ni(OH)_2$ as an adsorbent

Fig. 2 shows the powder XRD patterns for β-type $Ni(OH)_2$ (ICDD No. 01-076-8985) as a standard (a), synthesized $Ni(OH)_2$ (b) and purchased $NiCO_3$ as an adsorbent (c). The XRD pattern for the synthesized $Ni(OH)_2$ (b) was similar to that of the β-type $Ni(OH)_2$ although the observed crystallinity was slightly lower. The crystallinity of $NiCO_3$ (c) was also low. The specific surface areas for the $NiCO_3$ and synthesized $Ni(OH)_2$ as the adsorbent in this study were 203.3 and 208.1 $m^2\,g^{-1}$, respectively.

When the pH of the suspensions of $NiCO_3$ and $Ni(OH)_2$ changes, the surface charge of $NiCO_3$ and $Ni(OH)_2$ as the adsorbent may vary. The change in the surface charge affects the adsorption behavior of Au(III) complex ion on $NiCO_3$ and $Ni(OH)_2$. Therefore, the zeta potential of $NiCO_3$ and $Ni(OH)_2$ was measured in a pH range from 7 to 11. Fig. 3 shows the variation of zeta potential with pH and the variation of the adsorption proportions of Au(III) complex ions with pH. The adsorption proportion of Au(III) complex ions was calculated from the Eq. (1).

$$\text{Adsorption proportion } (\%) = \frac{[Au(III)]_0 - [Au(III)]}{[Au(III)]_0} \times 100 \quad (1)$$

where $[Au(III)]_0$ is the initial concentration of Au(III) complex ions in solution and $[Au(III)]$ is the concentration in solution at t (reaction time). The zeta potential of $NiCO_3$ (a) and $Ni(OH)_2$ (b) decreased with increasing pH. The isoelectric points for both $NiCO_3$ (a) and Ni(OH) (b) are around pH 10.5 and pH 11. Below pH 10.5 and pH 11, the surface charge is positive, this is generally interpreted that protons (H^+) may be adsorbed. On the other hand, the adsorption proportion of Au(III) complex ions decreased with increasing pH due to decrease in the positive charges dependent on pH. The variations of the zeta potential and the adsorption proportion with pH indicate that Au(III) complex ions with a negative charge and the surfaces of $NiCO_3$ (a) and $Ni(OH)_2$ (b) with positive charges interact electrostatically.

3.3. Variation with time of the adsorption proportion of Au(III) complex ions on $NiCO_3$ and $Ni(OH)_2$

Fig. 4 shows the variation with time of the adsorption proportion (%) of Au(III) complex ions on $NiCO_3$ (a) and $Ni(OH)_2$ (b) at pH 10. The initial Au concentrations were 10, 20 and 50 ppm. For reaction times from 0 to 700 min, the adsorption proceeded rapidly. The adsorption proportion increased with decreasing initial concentration of Au(III) complex ions. When adsorbing on $NiCO_3$ (a), the adsorption proportion at 1250 min appeared lower than that at 700 min. During the adsorption experiments, the pH shifted from pH 10 to pH 9. At 700 min, the pH was close to pH 9. When adsorbing on $Ni(OH)_2$ (b), the adsorption proportion from 1200 to 1500 min appeared lower than from 960 to 1200 min. At 960 min, the pH was close to 8.8. From this information, it appears that a decrease in the pH may cause an increase in the adsorption proportion of Au(III) complex ions. To confirm whether this hypothesis is correct, the amount of Au adsorbed on $NiCO_3$ and $Ni(OH)_2$ was plotted against the measured pH at each reaction time (after each measurement, the pH was readjusted to pH 10). The plot demonstrates a linear relationship in both cases (Fig. 5), indicating that the amount of Au adsorbed on $NiCO_3$ and $Ni(OH)_2$ decreases with increasing pH. Therefore, the amount of Au adsorbed on $NiCO_3$ and $Ni(OH)_2$ is sensitive to slight pH changes. This result indicates that changes in the surface charges of $NiCO_3$ and $Ni(OH)_2$ electrostatically control the adsorption of Au(III) complex ions.

3.4. Chemical state of Au adsorbed on $NiCO_3$ and $Ni(OH)_2$

To examine the chemical state of Au adsorbed on $NiCO_3$ and $Ni(OH)_2$, the Au L_3-edge XA spectra for standard materials and the solid samples were measured. Fig. 6 shows the Au L_3-edge XANES spectra for Au foil (a standard material of Au(0) with a Au—Au bond) (a), $K[AuCl_4]\cdot nH_2O$ (a standard material of Au(III) with a Au—Cl bond) (b), $Au(OH)_3$ (a standard material of Au(III) with a Au—O bond) (c), and the solid samples ($NiCO_3$ and $Ni(OH)_2$ adsorbing Au) (d and e). In the XANES spectra for $K[AuCl_4]\cdot nH_2O$ and $Au(OH)_3$, a white line appeared at 11.920 keV corresponding to the energy of an electronic transition from the $2p_{3/2}$ orbital to the 5d orbital. As the 5d orbital in Au(III) complex ion is not completely filled, the white line can be observed. As the 5d orbital in Au(0) and Au(I) complex ions is filled, in principle, no white line will be observed. The solid sample (d) shows a strong peak due to the white line and the peak intensity was the same as that of $Au(OH)_3$, suggesting that the Au adsorbed on $NiCO_3$ was present in the Au (III) state. In the $K[AuCl_4]\cdot nH_2O$ spectrum, a small peak appears at 11.935 keV. This peak is due to the Au-Cl bond [18]. As there is no

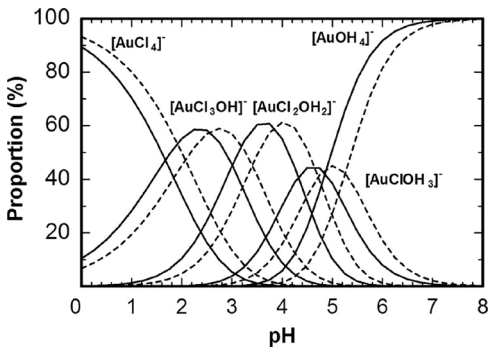

Fig. 1. Distribution of aqueous Au(III) complex ions versus pH. Au Source: $H[AuCl_4]$. Total Au concentration: − 20 ppm and − 50 ppm.

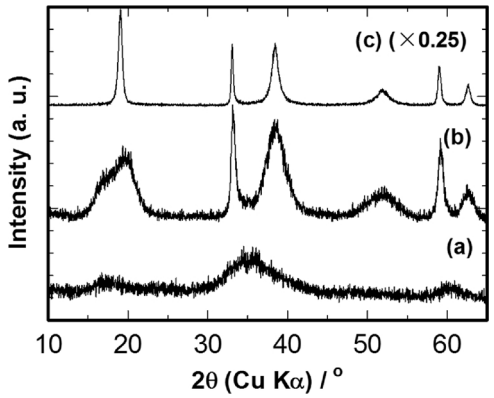

Fig. 2. Powder X-ray diffractograms of $NiCO_3$ as an adsorbent (a), synthesized $Ni(OH)_2$ as an adsorbent (b) and crystalline $Ni(OH)_2$ as a standard (c).

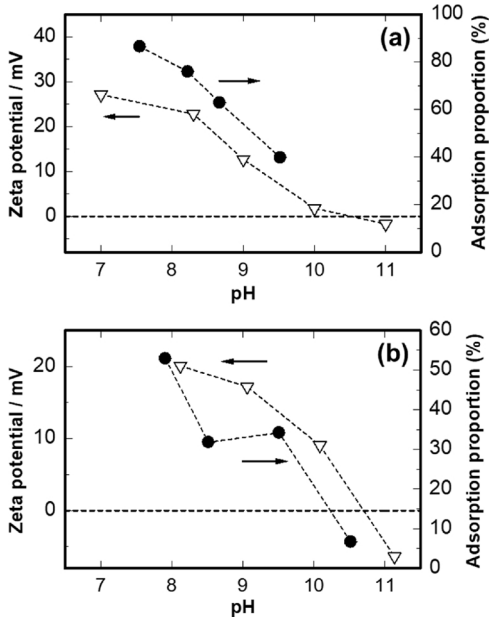

Fig. 3. Relationships between the amount of Au adsorbed on $NiCO_3$ (a) and $Ni(OH)_2$ (b) and its zeta potential. Initial Au concentration: 20 ppm. Reaction time: 24 h. Zeta potential: ▽. Adsorption proportion: ●.

similarly located peak in the solid sample spectrum, the Au adsorbed on $NiCO_3$ does not appear to have a Au-Cl bond. The XANES spectrum for the solid sample (d) is similar to that for $Au(OH)_3$ as a standard, suggesting that Au adsorbed on $NiCO_3$ consists of Au-O bonds. This result aligns with that in Fig. 1 that $[Au(OH)_4]^-$ is the adsorbed complex ion.

Unlike solid sample (d), the white line peak intensity for solid sample (e) significantly weakened and was lower than those for K$[AuCl_4]\cdot nH_2O$, $Au(OH)_3$ and solid sample (d). In addition, the peak appeared at ~11.950 keV as with Au foil. These facts suggest that a portion of the Au(III) complex ions adsorbed on $Ni(OH)_2$ may be reduced to Au(0). In the XANES spectrum for solid sample (e), no such peak appeared at 11.935 keV, suggesting that Au(III) complex ions adsorbed on $Ni(OH)_2$ do not also have an Au-Cl bond.

The Fourier transforms of the EXAFS oscillation extracted from the Au L_3-edge spectra for Au foil (a), K$[AuCl_4]\cdot nH_2O$ (b), $Au(OH)_3$ (c) and the solid sample (d) are shown in Fig. 7. The abscissa indicates the interatomic distance but the phase shift was uncorrected. In Fig. 7, the peak at 1.6 Å, the peak at 1.9 Å and the peaks at 2.5 and 3.0 Å can be assigned to Au−O, Au−Cl and Au−Au bonds, respectively. The Fourier transform of the EXAFS oscillation for the solid sample (d) was quite similar with that for $Au(OH)_3$, indicating that the above interpretation

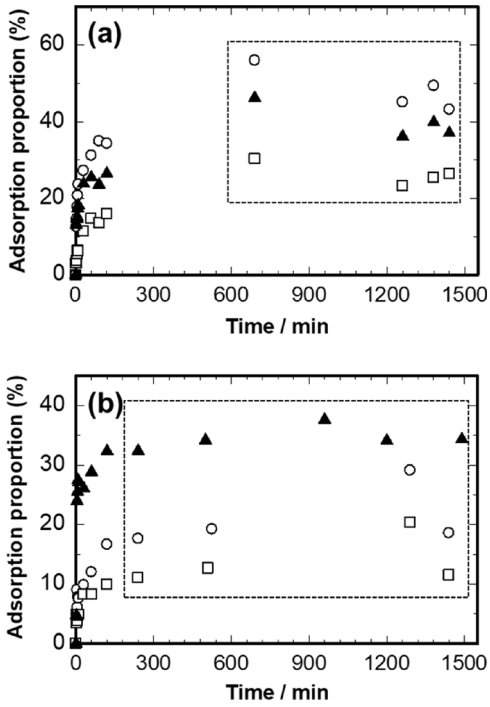

Fig. 4. Variation of adsorption proportion (%) of Au(III) complex ion on $NiCO_3$ (a) and $Ni(OH)_2$ (b) over time. Initial Au concentration; ○: 10 ppm, ▲: 20 ppm and □: 50 ppm.

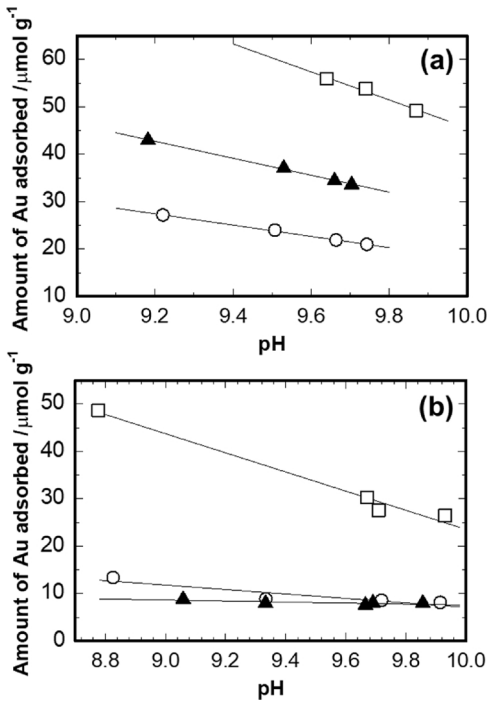

Fig. 5. Relationships between pH and amount of Au adsorbed on $NiCO_3$ (a) and $Ni(OH)_2$ (b). Plots surrounded by the dotted line in Fig. 4 were used. Initial Au concentration; ○: 10 ppm, ▲: 20 ppm and □: 50 ppm.

based on XANES spectra for the chemical state of Au adsorbed on $NiCO_3$ is reasonable. The EXAFS spectrum for the solid sample (e) was not obtained because of low sensitivity.

3.5. A model for adsorption of Au(III) complex ion on $NiCO_3$ and $Ni(OH)_2$

As shown in Fig. 1, Au is present as $[Au(OH)_4]^-$ complex ions in aqueous solutions above pH 7 in this study. The isoelectric points for

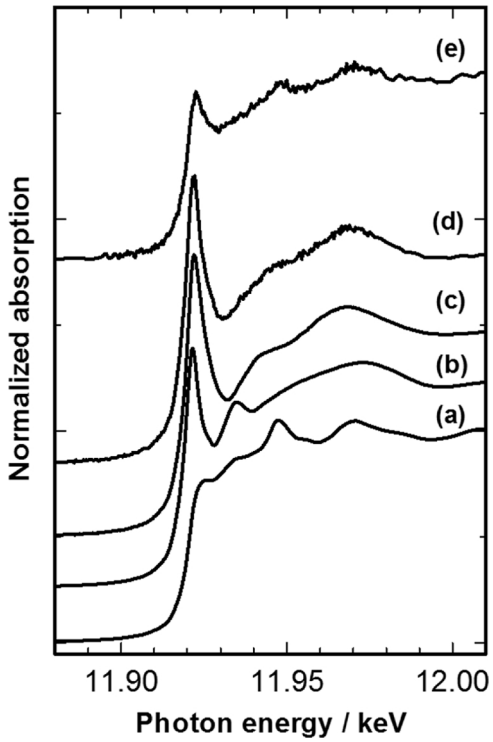

Fig. 6. Normalized Au L_3-edge XANES spectra for standard materials of Au and solid samples. Standard material: Au foil (a), $K[AuCl_4]{\cdot}nH_2O$ (b) and $Au(OH)_3$ (c), Samples: $NiCO_3$ adsorbing Au (d) and $Ni(OH)_2$ adsorbing Au (e).

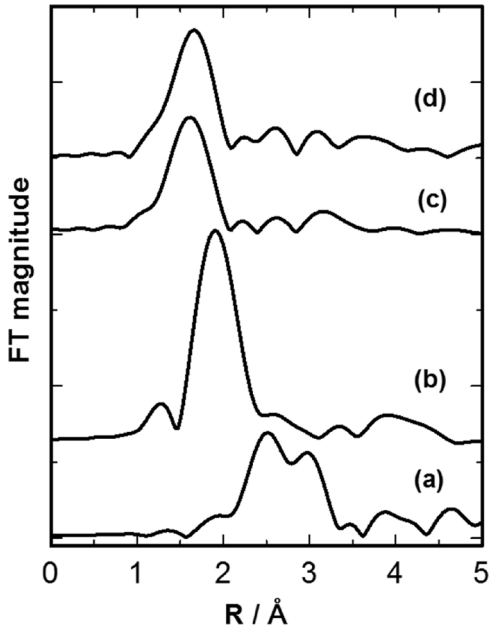

Fig. 7. The Fourier transform of EXAFS oscillation extracted from Au L_3-edge spectra. Standard material: Au foil (a), $K[AuCl_4]{\cdot}nH_2O$ (b) and $Au(OH)_3$ (c) Sample: $NiCO_3$ adsorbing Au (d).

$NiCO_3$ and $Ni(OH)_2$ are near pH 10.5 and pH 11, respectively. As the zeta potentials of $NiCO_3$ and $Ni(OH)_2$ were positive below pH 10.5, H^+ and/or Ni^{2+} may be adsorbed on $NiCO_3$ and $Ni(OH)_2$ depending on the pH. Therefore, the zeta potential increases with decreasing pH, indicating that the amount of positive charges increases with decreasing pH as shown in Fig. 3. Consequently, $[Au(OH)_4]^-$ is electrostatically adsorbed on $NiCO_3$ and $Ni(OH)_2$ with decreasing pH as shown in Fig. 8a. This electrostatic interaction between $[Au(OH)_4]^-$ with

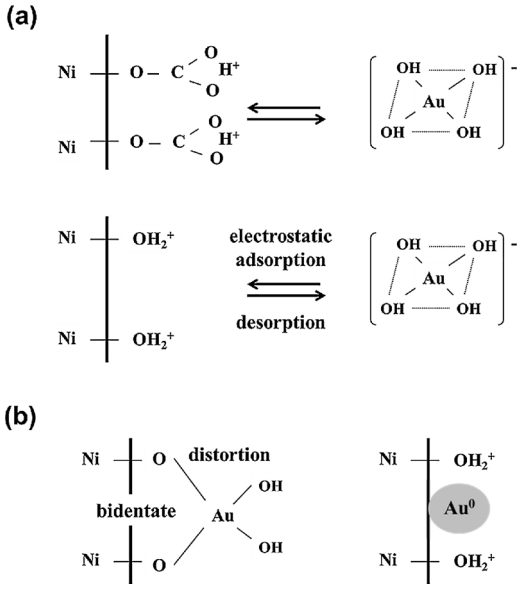

Fig. 8. Proposed models for the adsorption behavior of Au(III) complex ion on $NiCO_3$ and $Ni(OH)_2$. First step ($NiCO_3$ and $Ni(OH)_2$)(a) and Second step ($Ni(OH)_2$)(b).

Table 1
The adsorption experiment data of Au(III) complex ion onto the $NiCO_3$ after 24 h.

pH	Adsorption proportion (%)	Amount of Au/μmol	Coverage (%)
7.29	86.7	39.4	1.82
8.16	79.4	35.5	1.64
8.78	61.7	27.5	1.27
9.66	37.0	17.2	0.797

Calculating formula of the coverage coverage (%) $= \frac{a \times N_A \times b}{c \times d} \times 100$.

a: amount of adsorbed Au (mol)
b: occupation area of a Au(III) complex ion (m^2)
c: specific surface area of $NiCO_3$ ($m^2\ g^{-1}$)
d: amount of $NiCO_3$ used at the adsorption experiment (g)
N_A: Avogadro's number (mol^{-1}).

negative charge and the surface of $NiCO_3$ and $Ni(OH)_2$ with positive charges is the initial adsorption mode.

Table 1 represents the coverage (%) of the specific surface area by $[Au(OH)_4]^-$ complex ions adsorbed on $NiCO_3$. The $[Au(OH)_4]^-$ complex has a 4-coordinate square planar structure and its Au—O bond distance is 1.98 Å. As the distance between OH^- ligands is 2.80 Å, one $[Au(OH)_4]^-$ complex ion can be assumed to occupy $7.84 \times 10^{-20}\ m^2$. The maximum coverage was lower than 2%. This result suggests that Au(III) complex ions are adsorbed on $NiCO_3$ as isolated molecules (monodisperse adsorption).

As the chemical state of the $[Au(OH)_4]^-$ complex adsorbed on $NiCO_3$ did not change and the quantity of $[Au(OH)_4]^-$ complex ions adsorbed at a given pH attained a constant value after a given time, only an electrostatic interaction appears to control the adsorption of Au (III) complex ions on $NiCO_3$, which approaches an adsorption/desorption equilibrium depending on pH. On the other hand, a fraction of the $[Au(OH)_4]^-$ complex ions adsorbed on $Ni(OH)_2$ were converted to Au(0). The reduction of the Au(III) complex ions to Au(0) has been previously observed during the adsorption of Au(III) complex ions on metal sulfides [19–22]. Although some works have shown a reduction of Au(III) complex ions adsorbed on silicates [23,24], oxides and hydroxides [8,9,25] to Au(0), the mechanism has not been elucidated to date. Some researchers carried out adsorption experiments of Au(III) complex ion on silicate minerals immediately after crushing and found that the adsorbed Au(III) complex ions were reduced. They suggested that the reduction may have been due to radicals generated by the

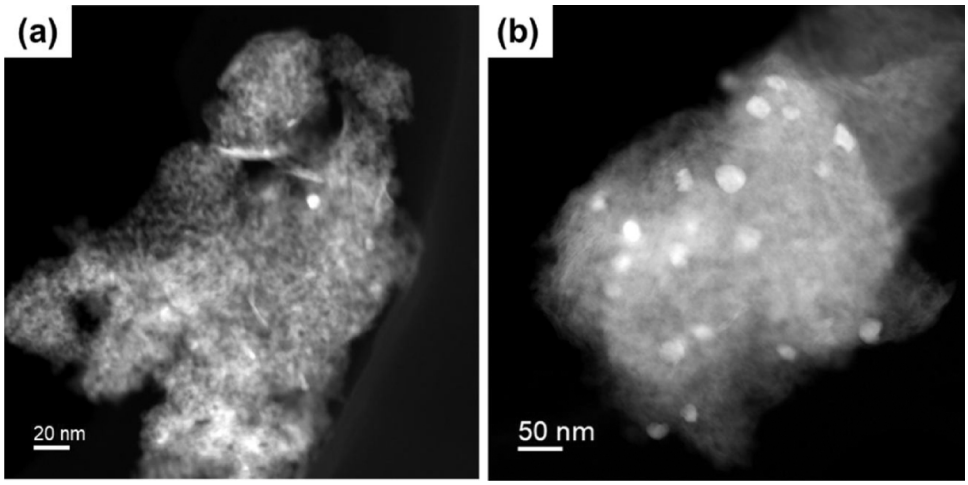

Fig. 9. TEM image for the Au/NiO prepared from $NiCO_3$ (a) and $Ni(OH)_2$ (b).

crushing of silicate minerals or hydrogen molecules generated by a reaction between the radicals and water molecules. Other researchers previously found that when Au(III) complex ions were coprecipitated with aluminum hydroxide ($Al(OH)_3$), some of the Au(III) complex ions were reduced to Au(0) in the absence of a specific reducing reagent [25]. They proposed a reduction mechanism as follows. When an Au (III) complex ion is adsorbed bidentately between two hydroxyl groups of the Au(III) complex ion and two hydroxyl groups of the surface of Al $(OH)_3$ through a condensation reaction by the formation of Al-O-Au bonds, the coordination structure of the adsorbed Au(III) ion may be distorted because of the steric regulation of hydroxyl groups on Al $(OH)_3$, and the oxidation/reduction potential of the Au(III) ion in the $[Au(OH)_4]^-$ complex ion may be changed (the authors reported the existence of the bidentate Au(III) complex ion adsorbed on CeO_2 by EXAFS analysis [26]). Consequently, the Au(III) ion may be reduced by H_2O according to the following reaction Eq. (2) [27].

$$Au^{3+}\ (\text{distorted on } Al(OH)_3) + 3/2H_2O \rightarrow Au(0) + 3/4O_2 + 3H^+ \quad (2)$$

In the adsorption of $[Au(OH)_4]^-$ complex ions on $Ni(OH)_2$ in this study, there is no specific reducing reagent like that with $Al(OH)_3$. Therefore, $[Au(OH)_4]^-$ adsorbed electrostatically on $Ni(OH)_2$ and then a surface complex which coordinates bidentately may be formed. The distorted $[Au(OH)_4]^-$ on $Ni(OH)_2$ may be spontaneously reduced by H_2O molecules according to Eq. (1), as shown in Fig. 8b.

3.6. TEM observation and implications to supported Au catalyst

Fig. 9 shows the TEM image for the catalysts (Au/NiO) prepared from $NiCO_3$ (a) and $Ni(OH)_2$ (b), respectively. The particle sizes for Au were 6.70 ± 2.13 nm and 31.1 ± 11.0 nm for the Au/NiO prepared from $NiCO_3$ and $Ni(OH)_2$, respectively. As well known, the catalytic activity strongly depends on the Au particle size and it is important to control the particle size within several nm. From the result of this study, it is preferable to prepare the catalyst precursor by using $NiCO_3$ rather than by using $Ni(OH)_2$ because the size of Au particle can be controlled within several nm when $NiCO_3$ is used as the supported compound, on the other hand, the size exceeds several nm when $Ni(OH)_2$ is used. In addition, relative large Au particle was observed in the precursor whose support compound was $Ni(OH)_2$ and the Au particle grew to larger one by heating the precursor at 300 °C. The results obtained in this study demonstrate that the detailed characterization of precursor is essential to synthesize metal oxide-supported Au catalysts with higher catalytic activity.

4. Conclusion

Supported Au has been used as a catalyst for the effective oxidation of CO to CO_2. In our prior work concerning the precursor of a Au/NiO catalyst prepared by the coprecipitation method (CP method), we noted that when Au(III) complex ion is coprecipitated with $Ni(OH)_2$ (NaOH solution was used as a coprecipitating reagent), the coprecipitated Au (III) complex ions were reduced to Au(0), whereas the Au(III) complex ions coprecipitated with $NiCO_3$ were not reduced (Na_2CO_3 solution was used as a coprecipitating reagent).

In this study, to elucidate the variation of the chemical states of Au in the precursor, the adsorption behavior of Au(III) complex ions on $NiCO_3$ and $Ni(OH)_2$ was investigated as a model reaction for the precursor preparation. Accordingly, different adsorption mechanisms of Au (III) complex ion are proposed. Our results suggest that when the precursor is prepared by the CP method, the carrier of Au(III) complex ions in the precursor, such as $NiCO_3$ and $Ni(OH)_2$, considerably affects the chemical state of the Au(III) complex ion.

Acknowledgements

This work was financially supported by Japan Science and Technology Agency-Advanced Low Carbon Technology Research and Development Program (JST-ALCA; grant number: 11102798). The synchrotron radiation experiments were performed at the BL14B2 in SPring-8 with the approval of JASRI(2014B1897, 2015A1702).

References

[1] M. Haruta, T. Kobayashi, H. Sano, N. Yamada, Chem. Lett. 16 (2) (1987) 405–408.
[2] S. Wang, Y. Wang, J. Jiang, R. Liu, M. Li, Y. Wang, Y. Su, B. Zhu, S. Zhang, W. Huang, S. Wu, Catal. Commun. 10 (2009) 640–644.
[3] M. Haruta, J. New Mater. Electrochem. Syst. 7 (2004) 163–172.
[4] L. Arab, M. Boutahara, B. Djellouli, T. Dintzer, V. Pitchon, Appl. Catal. A 475 (2014) 446–460.
[5] S. Scire, C. Crisafulli, P.M. Riccobene, G. Patane, A. Pistone, Appl. Catal. A 417–418 (2012) 66–75.
[6] H. Ando, D. Kawamoto, H. Ohashi, Y. Kobayashi, T. Ishida, Y. Okaue, M. Tokunaga, T. Yokoyama, Adv. X-Ray Chem. Anal. Jpn. 47 (2016) 111–118.
[7] I.V. Fedoseyava, G.V. Zvonareva, Geochim Int. 25 (1988) 115–119.
[8] I. Berrodier, F. Farges, M. Benedetti, M. Winterer, G.E. Brown Jr., M. Deveughele, Geochim. Cosmochim. Acta 68 (2004) 3019–3042.
[9] H. Ohashi, H. Ezoe, Y. Okaue, Y. Kobayashi, S. Matsuo, T. Kurisaki, A. Miyazaki, H. Wakita, T. Yokoyama, Anal. Sci. 21 (2005) 789–793.
[10] O.N. Karasyova, L.I. Ivanova, L.Z. Lakshtanov, L. Lövgren, S. Sjöberg, Aquat. Geochem 4 (1998) 215–231.
[11] H. Schötza, I. Schötza, Z. Anorg. Allg. Chem. 245 (1940) 59–66.
[12] D. Kawamoto, H. Ando, H. Ohashi, Y. Kobayashi, T. Honma, T. Ishida, M. Tokunaga, Y. Okaue, S. Utsunomiya, T. Yokoyama, Bull. Chem. Soc. Jpn. 89 (2016) 1385–1390.
[13] B. Ravel, M. Newville, J. Synchrotron Radiat. 12 (2005) 537–541.

[14] C.F. Baes Jr., R.E. Mesmer, The Hydrolysis of Cations, John Wiley & Sons, New York, 1976.
[15] J.A. Peck, C.D. Tait, B.I. Swanson, G.E. Brown Jr: Geochim, Cosmochim. Acta 55 (1991) 671–676.
[16] P.J. Murphy, M.S. Lagrange, Geochim. Cosmochim. Acta 62 (1998) 3515–3526.
[17] M.L. Machesky, W.O. Andrade, A.W. Rose, Geochim. Cosmochim. Acta 55 (1991) 769–776.
[18] X. chen, W. Chu, D. Chen, Z. Wu, A. Marcelli, Z. Wu, Chem. Geol. 268 (2009) 74–80.
[19] L.M. Maddox, G.M. Bancroft, M.J. Scaini, J.W. Lorimer, Am. Mineral 83 (1998) 1240–1245.
[20] M.J. Scaini, G.M. Bancroft, S.W. Knipe, Geochim. Cosmochim. Acta 61 (1997) 1223–1231.
[21] Y. Mikhlin, A. Romanchenko, M. Likhatski, A. Karacharov, S. Erenburg, S. Trubina, Ore Geol. Rev. 42 (2011) 47–54.
[22] L. Makhova, Y. Mikhlin, A. Romanchenko, Nucl. Instrum. Methods Phys. Res. Sect. A 575 (2007) 75–77.
[23] S. Mohammadnejad, J.L. Provis, J.S.J. van Deventer, J. Colloid Interface Sci. 389 (2013) 252–259.
[24] D. Feng, J.L. Provis, J.S.J. van Deventer, Hydrometallurgy 134–135 (2013) 32–39.
[25] T. Yokoyama, Y. Matsukado, A. Uchida, Y. Motomura, K. Watanabe, E. Izawa, J. Colloid Interface Sci. 233 (2001) 112–116.
[26] T. Yokoyama, Abstract of an Annual Meeting of XAFS (Fukuoka), (2006).
[27] C.H. Gammons, Y. Yu, A.E. Williams-Jones, Geochim. Cosmochim. Acta 61 (1997) 1971–1983.